Supporting Information

Pyrite FeS$_2$ microspheres anchoring on reduced graphene oxide aerogel as an enhanced electrode material for sodium ion batteries

Weihua Chen, [a,b,*] Shihan Qi,[a] Linquan Guan,[a] Chuntai Liu,[b] Shizhong Cui,[c] Changyu Shen[b] , Liwei Mi [c,*]

a.   College of Chemistry and Molecular Engineering, Zhengzhou University, Zhengzhou, 450001, P. R. China. E-mail: chenweih@zzu.edu.cn.

b.   National Engineering and Research Center for Adv. Polymer Processing Technology, Zhengzhou University, Zhengzhou, 450001 P. R. China

c.   Center for Advanced Materials Research, Zhongyuan University of Technology, Zhengzhou, 450007, P.R. China. E-mail: mlwzzu@163.com.
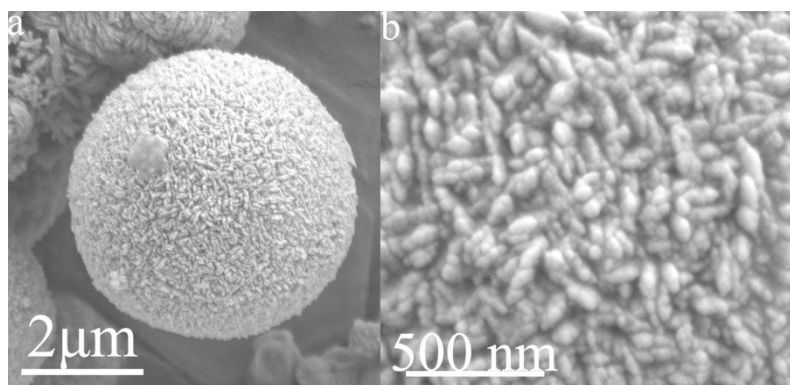
1. The morphology of pure FeS$_2$ microsphere

Fig S1. The SEM images of (a) single FeS$_2$ micro sphere and (b) the surface of FeS$_2$ micro sphere

2. The role of SiO$_2$ nanoparticles in as-synthesized composite material

2.1 The method of removing SiO$_2$ nano-particles

2.1.1 HF method

About 50 mg FeS$_2$@rGO-A composite material was added into 100 mL 10% HF aqueous solution (v/v), followed by stirring for 30 min at ambient temperature. Then, the HF treated product was collected by centrifugation, washed with DI water and alcohol for several times. The final product was dried at 80˚C overnight.

2.1.2 NaOH method

About 50 mg FeS$_2$@rGO-A hybrid material was added into 100 mL 1M NaOH solution, followed by stirring for 2 h at 70 ˚C by using water bath. The NaOH treated product was collected by centrifugation, washed with DI water and alcohol for several times to remove the organic solvent. The final product was dried at 80 ˚C overnight.

2.1.3 Material characterization of the above two samples

Scanning electron microscope (SEM), energy dispersive X-ray spectroscopy (EDS) and powder X-ray diffraciton (XRD) were carried out to characterize the morphology, elemental distribution and crystal phase information, respectively.
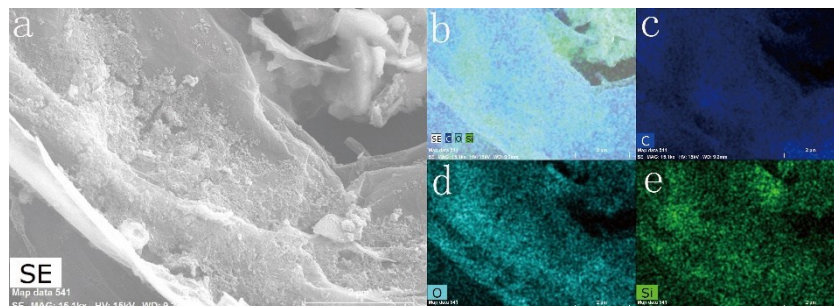
2.2 Results and Discussion

Fig. S2. (a) SEM image of a graphene sheet in our untreated sample (550 ˚C) and the nano-particles on it, (b-e) EDS mappings of this region.
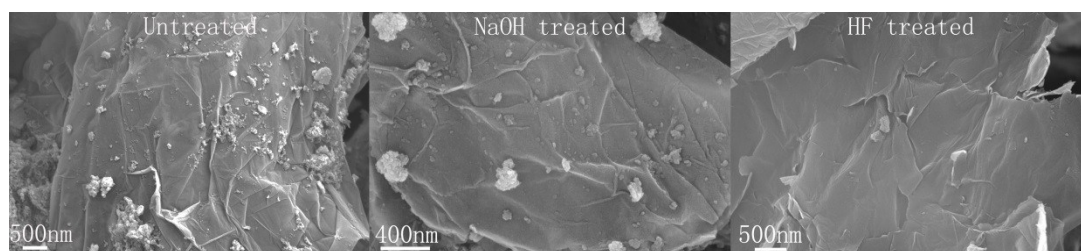

Fig. S3. The SEM images of (a) untreated sample, (b) NaOH treated sample, (c) HF treated sample (this 3 samples were thermal treated at 750 ˚C).
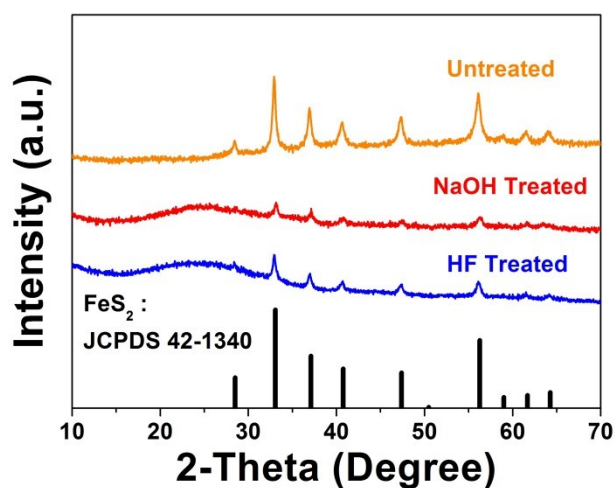

Fig. S4. The XRD profiles of untreated sample, NaOH treated sample and HF treated sample.
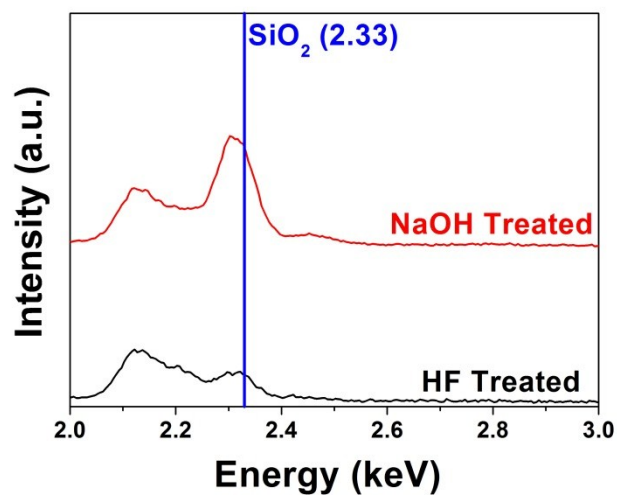
Fig. S5. EDS profiles of NaOH treated sample and HF treated sample.

Table. S1. The Si elemental contents of different samples (atom content)

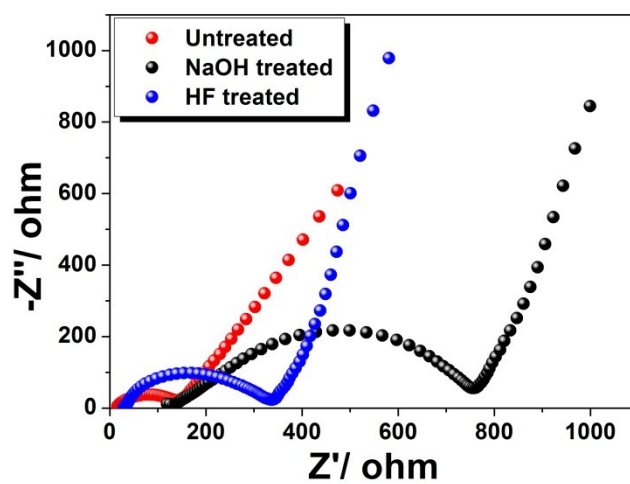| Method of treatment	Si elemental content/ %
Untreated	0.38
HF treated	0.05
NaOH treated	0.11

Fig. S6. Nyquist plots of untreated sample, NaOH treated sample and HF treated sample.
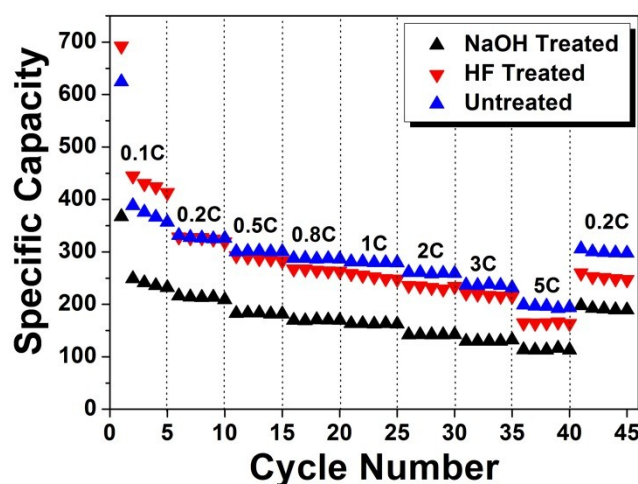
Fig. S7. Rate performance of untreated sample, NaOH treated sample and HF treated sample.

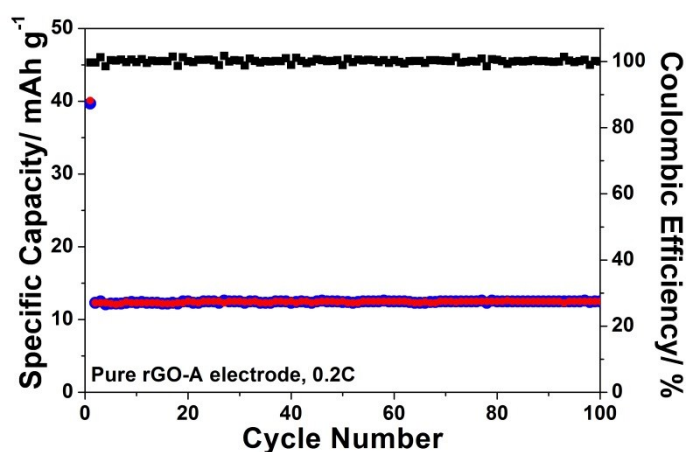## 3. Electrochemical performances of pure rGO-A electrode

Fig. S8. Cyclic performance of pure rGO-A at 0.2C.

4. The calculation of the content of active material

The content of active material was calculated by followed equation:

$$C = \frac{R_1 - R_2}{0.665 - R_2}$$ Equation S1

where R_1 is the mass residue rate of composite, R_2 is the mass residue rates of rGO-A(SiO_2), 0.665 is the mass residue rate of pristine FeS_2 (the FeS_2 thermal treated final product is Fe_2O_3), C is the content of active material in the composite.

5. The calculation of sodium ion diffusion coefficients

The sodium-ion diffusion coefficient can be obtained from EIS results. The calculation formula is shown as follows:

$$D = \frac{R^2 T^2}{2A^2 n^4 F^4 C^2 \sigma^2} ,$$
Equation S2

where R represents the gas constant, T is the test temperature, A is the surface area of our electrode, F is the Faraday constant, n represents the number of electrons per molecule attending the charge-discharge reaction, C is the concentration of sodium ion in our composite electrode, and σ is the slope of the line Z' - $\omega^{-1/2}$ (shown in Fig. 4(e)).
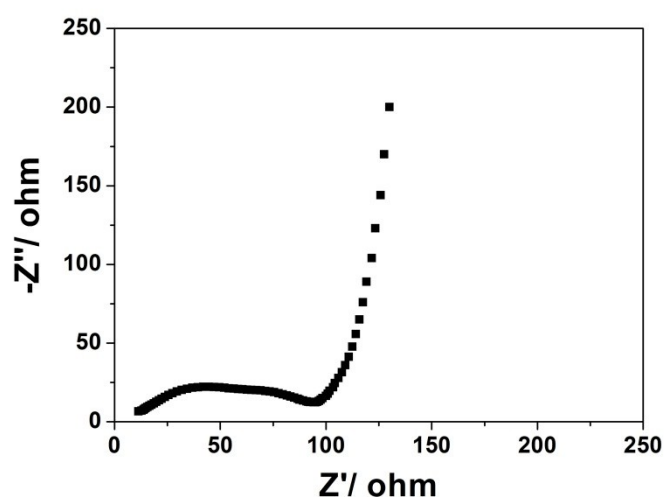
6.The Nyquist plots of rGO-A electrode

Fig. S9. Nyquist plot of pure rGO-A electrode.
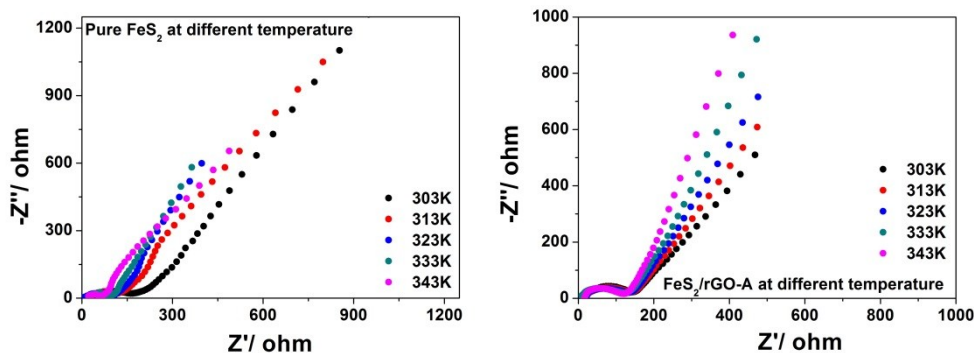
7. The calculation of apparent activation energy

Fig. S10. Nyquist plots of (a) pure FeS_2 electrode and (b) FeS_2/rGO-A electrode at different temperatures.

We also calculated the activation energy (Ea) from the EIS data at different temperatures using the equations: $i_0 = RT/nFR_{ct}$ (Equation S3) and $i_0 = A\exp(-E_a/RT)$ (Equartion S4), where A is a temperature-independent coefficient, R is the gas constant, T is the absolute temperature, n is the number of transferred electrons, and F is the Faraday constant.

8. The electrochemical performance of FeS_2/rGO-A composite tested in a large operation voltage range
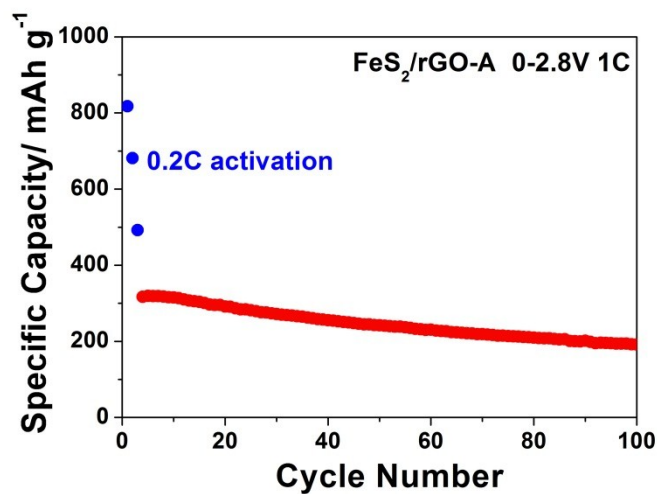

Fig. S11. Cyclic performance of FeS_2/rGO-A in the voltage range of 0-2.8 V.

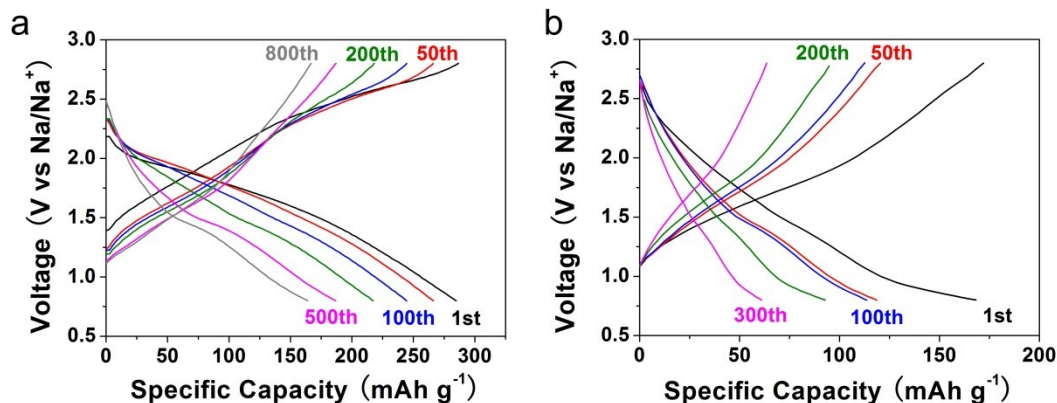## 9. The charge and discharge profiles of FeS$_2$/rGO-A and pure FeS$_2$

Fig. S12. Charge and discharge profiles of (a) FeS$_2$/rGO-A electrode and (b) pure FeS$_2$ electrode at different cycles (at 1C).

10. Loading amounts and thicknesses of FeS$_2$/rGO-A electrodes and and FeS$_2$ electrodes.

Table. S2. Loading amounts of FeS$_2$/rGO-A electrodes and pure FeS$_2$ electrodes.

No.	1	2	3	4	5	6	7	8	9	10	Average
loading amount of FeS$_2$/rGO-A (mg cm^{-2})	6.42	5.91	6.01	6.11	6.52	6.01	6.01	6.32	6.22	6.42	6.19
loading amount of FeS$_2$ in FeS$_2$/rGO-A (mg cm^{-2})	5.07	4.67	4.75	4.83	5.15	4.75	4.75	4.99	4.91	5.07	4.89
loading amount of FeS$_2$ (mg cm^{-2})	7.85	7.95	7.44	7.95	7.64	7.95	8.05	7.75	7.85	7.54	7.80

The loading amount of the FeS$_2$/rGO-A electrode was kept at about 4.9 mg cm^{-2} and the thickness of electrode materials was about 45 μm. Besides, for FeS$_2$ electrode, the values were about 7.8 mg cm^{-2} and 40 μm, respectively.

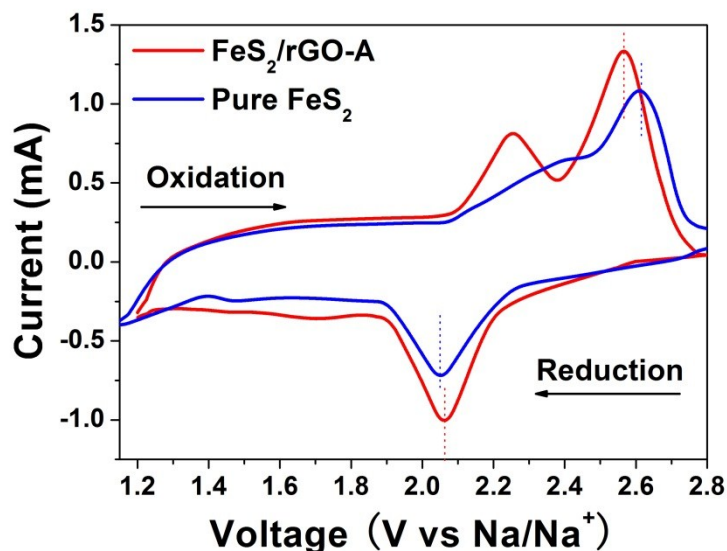## 11. CV profiles of FeS$_2$/rGO-A electrode and pure FeS$_2$ electrode

Fig. S13 CV profiles of FeS$_2$/rGO-A electrode and pure FeS$_2$ electrode of the 2nd cycle at a scan rate of 0.2 mV s^{-1}.

As shown in Fig. S13, there are one reduction peak and two oxidation peaks on the CV profile of FeS$_2$/rGO-A, corresponding to the sodiation and desodiation processes, respectively. The two oxidation peaks may correspond to the desodiation processes of two different Na$^+$ ions. There is only one obvious oxidation peak on the CV profile of pure FeS$_2$ because only about one Na$^+$ ion extracts out of FeS$_2$. Obviously, the potential difference of FeS$_2$/rGO-A between oxidation peaks and reduction peak is smaller than the one of pure FeS$_2$, suggesting that FeS$_2$/rGO-A suffers a smaller polarization. This outcome indicates that the conductivity of FeS$_2$ is lower than FeS$_2$/rGO-A's.

Table. S3. Comparison of electrochemical performance of FeS_2/rGO-A in this work with reported related materials in Sodium Ion battery.

Sample	Current	Cyclic Performance	Ref
FeS_2/rGO-A	900 mA/g	decay rate of 0.051% per cycle over 800 cycles (181.0 mAh/g reserved)	**This work**
	200 mA/g	decay rate of 0.091% per cycle over 200 cycles (238.4 mAh/g reserved)	
Ultrafine FeS_2 Nanocrystals	100 mA/g	decay rate of 1.2% per cycle over 30 cycles	*ACS Nano*[1] **2015**
PEO-MoS_2	50 mA/g	decay rate of 0.489% per cycle over 70 cycles (148 mAh/g)	**Nano Energy**[2] **2015**
MoS_2@C-CMC	80 mA/g	286 mAh/g after 100 cycles	**Adv.Energy Mater.**[3] **2016**
WS_2/CNT-rGO aerogel	200 mA/g	259.2 mAh/g after 100 cycles	**Adv.Energy Mater.**[4] **2016**
Hollow NiS spheres	100 mA/g	decay rate of 0.54% per cycle over 50 cycles	**Adv. Funct. Mater.**[5] **2016**
CoS_2-CoS-G microspheres	200 mA/g	decay rate of 0.31% per cycle over 100 cycles	**Nano Energy**[6] **2016**

1. A. Douglas, R. Carter, L. Oakes, K. Share, A.P. Cohn and C.L. Pint, Acs Nano, 2015, **9(11)**, 11156.

2. Y.F. Li, Y.L. Liang, F.C.R. Hernandez, H.D.Yoo, Q.Y. An, Y. Yao, Nano Energy, 2015, **15**, 453.

3. X.Q. Xie , T. Makaryan , M.Q. Zhao , K.L.V. Aken , Y. Gogotsi and G.X. Wang, *Adv. Energy Mater.*, 2016, **6**, 1502161.

4. Y. Wang, D.Z. Kong, W.H. Shi, B. Liu, G.J. Sim, Q. Ge and H.Y. Yang, *Adv. Energy Mater.*,2016, **6**, 1601057.

5. D. Zhang, W.P. Sun, Y. Zhang, Y.H. Dou, Y.Z. Jiang and S.X. Dou, *Adv. Funct. Mater.*, 2016, **26**, 7479.

6. J.S. Cho, J.M. Won, J.K. Lee, Y.C. Kang, *Nano energy*, 2016, **26**, 466.